Removing Critical Errors for DFT Applications to Transition-Metal Nanoclusters: Correct Ground-State Structures of Ru Clusters

ARTICLE *in* THE JOURNAL OF PHYSICAL CHEMISTRY B · JANUARY 2006

Impact Factor: 3.3 · DOI: 10.1021/jp0555347 · Source: PubMed

THE JOURNAL OF PHYSICAL CHEMISTRY B LETTERS

2005, *109,* 23113−23117
Published on Web 11/22/2005

Removing Critical Errors for DFT Applications to Transition-Metal Nanoclusters: Correct Ground-State Structures of Ru Clusters

L.-L. Wang and D. D. Johnson*

Department of Materials Science and Engineering, University of Illinois at Urbana-Champaign, 1304 West Green St., Urbana, Illinois 61801, and Frederick Seitz Materials Research Laboratory, University of Illinois at Urbana-Champaign, 104 South Goodwin Ave., Urbana, Illinois 61801

Received: September 28, 2005; In Final Form: November 1, 2005

As ruthenium plays an important role in heterogeneous catalysis, understanding the structural and electronic properties of Ru clusters is crucial to advancement of technology. Because of its efficiency, density functional theory (DFT) calculations are often utilized in nanoscience, but careful validation is necessary. Recently, small, nonmetallic Ru_n clusters were reported by Zhang et al. [*J. Phys. Chem. B* **2004**, *108*, 2140] to form unusual square and cubic ground-state structures within DFT by treating the exchange-correlation (XC) functional at the level of general-gradient-corrected approximation (GGA). For such clusters, we show that the calculated, energetically preferred structures are sensitive to which XC functional is used and whether relativistic effects are included. We find that a hybrid XC functional with partially exact exchange, such as PBE0, corrects the Ru_2 magnetic moment, bond length, and dissociation energy in agreement with experiment and high-level quantum chemistry calculations and changes the Ru_4 ground-state structure to a tetrahedron, instead of a square. The change in structural preference is explained by the corrections to the electronic structure of a Ru atom, where the relative position of majority spin s level is shifted with respect to e_g levels. We also find that standard nonrelativistic DFT-GGA gives similar results to relativistic DFT-PBE0, i.e., relative shifting of s level, but not for the right reasons. Our results again stress the need to validate an XC functional before application to transition-metal nanoclusters.

Introduction

Because of their crucial roles in heterogeneous catalysis, transition-metal nanoclusters have been intensively studied in both theory and experiment for the past decade. Among them, the Ru cluster is unique. For example, when alloyed with Pt on a support, it drastically reduces poisoning of Pt with carbon monoxide.[1] Thus, a deeper understanding of the properties of the Ru cluster can provide us with better design of catalysts—but only if the correct ground states and electronic structures are obtained. Recently, a study of the Ru cluster using density functional theory (DFT) calculation and treating the exchange-correlation (XC) functional at the level of generalized-gradient-approximation (GGA) has been reported by Zhang et al.[2] They found that Ru clusters with 55 or fewer atoms prefer structures with a maximum number of simple cubic and square structures. However, this structural habit is highly unusual for mid-transition-metal clusters and is counter to the simple Debye−Hückel (tight-binding) arguments. Therefore, further DFT investigations are needed that are validated by comparison to available experimental data or high-level quantum chemistry methods that treat electron correlation more accurately.

In this letter, we present the DFT results for structural and electronic properties of free-standing, small Ru_n cluster ($n = 2-4$) for different XC functionals and for nonrelativistic and scalar relativistic cases—both are commonly used in quantum chemistry and solid-state studies—and show that the DFT energetically preferred structures are sensitive to both choice of XC functional and relativistic approximations. We compare our results with experimental data, other DFT results, and the results from high-level quantum chemistry methods published in the past decade. With a hybrid XC functional that includes partially exact exchange, such as PBE0,[3,4] DFT gives the ground-state magnetic moment, bond length, and dissociation energy of Ru_2 in good agreement with experiment and high-level quantum chemistry calculations. Moreover, the ground-state structure of Ru_4 is predicted to be a tetrahedron by PBE0, not a square. We explain the origin of such a preference from the electronic structure of a single Ru atom. In addition, we show that nonrelativistic DFT-GGA gives similar structural properties to the correct scalar relativistic DFT-PBE0 results, i.e., "the right results for the wrong reasons". Importantly, we have validated the results in several solid-sate and quantum chemistry codes, in which all codes obtain the same results for a fixed choice of XC functionals. Our results, again, stress the need for validating approximate XC functionals within the DFT method before application in nanoscience.

Computational Methods

Because of the open 4d shell of the Ru atom, a theoretical study of Ru clusters is challenging. A large number of electronic states of different spin multiplicities can arise from the strong electron-correlation effects. So, the electronic structure of

* duanej@uiuc.edu.

10.1021/jp0555347 CCC: $30.25

TABLE 1: Magnetic Moment (M), Bond Length (r_e), and Dissociation Energy (D_e) for Ru Dimer (Ru_2)[a]

	M (μ_B)	r_e (Å)	D_e (eV)
MRSDCI[29]	6	2.36	2.00
NWC PBE0(SR)	6	2.26	1.98
VASP PW91(SR)	4	2.11	3.78
NWC PW91(SR)	4	2.15	3.25
VASP PW91(SR)[2]	4	2.04	4.04
BP(NR)[32]	6	2.33	2.56
LDA(NR)[33]	6	2.41	2.70

[a] We note that the use of ultrasoft pseudopotential (USPP) in ref 2 did not include semicore 4s4p states as valence state; hence, the larger errors for r_e and D_e compared to the present results (see Computational Methods section).

nonmetallic Ru cluster is multiconfigurational in nature, and a careful treatment of electron-correlation and relativistic (Darwin and mass-velocity) effects is necessary (here, we ignore spin−orbit coupling, i.e., we consider scalar relativistic approximation).

It is known that DFT with standard XC functional (LDA and GGA) always underestimates band gap for semiconductors and HOMO−LUMO gap for small molecules. For a nonmetallic system with strongly correlated electrons, such as a transition-metal oxide, DFT with standard XC functionals can give qualitatively incorrect results, even predicting a metal instead of an insulator for many cases.[5] Such problems are due to the unphysical self-interaction of electrons within DFT. Unlike the Fock operator in the Hartree−Fock (HF) equation, which removes the electron self-interaction term properly, the normal XC potential in the Kohn−Sham (KS) equation does not. To overcome this problem, one can perform a direct subtraction of the electron self-interaction for each KS orbital[6,7] or use the exact exchange functional obtained by the optimized effective potential method.[8−11] Alternatively, the XC functional can be constructed to include part of the HF exchange, which is known as the hybrid XC functional or adiabatic connection model.[12−14] PBE0 is one of the widely used hybrid XC functionals, which includes 25% of the HF exchange in PBE.[3,4] PBE0 has been shown to produce chemical accuracy for various systems and overcome the unphysical self-interaction of electron in DFT,[15] as in recent application to transition-metal organics[16−19] and oxide.[20]

For our DFT calculations, we used a variety of DFT implementations to help identify the origin of structural errors in Ru clusters. We used both periodic and open boundary conditions. For periodic boundary conditions, we used the plane-wave basis and the projector-augmented-wave (PAW) method as implemented in VASP[21,22] and the all-electron, full-potential augmented plane-waves as implemented in FLAIR.[23,24] For open boundary conditions, we used the Gaussian basis and the relativistic effective core potentials as implemented in NWChem[25,26] and the all-electron, full-potential Gaussian basis as implemented in NRL-MOL.[27,28] In both VASP and NWChem, in addition to the outermost valence 4d5s states, the semicore 4s4p states were also treated as valence state—otherwise, as shown by an earlier study,[29] it leads to an unreasonably short Ru−Ru bond length.

Results and Discussion

In Table 1, we list the results for the Ru dimer (Ru_2) using DFT with different XC functionals and based on scalar relativistic (SR) and nonrelativistic (NR) approximations, together with the previously published results using both DFT and wave function-based quantum chemistry methods. The multireference singles and doubles configuration interaction (MRSDCI) gives the total magnetic moment (M) of 6 μ_B, bond length (r_e) of 2.36 Å, and dissociation energy (D_e) of 2.00 eV,[29] agreeing with 2.0 eV from experiment.[30] MRSDCI has a better treatment for the strong electron-correlation effect than DFT, which is manifested by the accurate prediction of the dissociation energy. So, without experimental data on magnetic moment and bond length for the Ru dimer, the MRSDCI results should be regarded as the benchmark for the DFT calculations. For PBE0-(SR), shown in Table 1, the magnetic moment, bond length, and dissociation energy of 1.98 eV all agree well with the MRSDCI and experimental results. Also shown in Table 1, PW91(SR) gives overly small magnetic moment and bond length, and a dissociation energy too large by a factor of 2 (we include results from ref 2 for comparison[31]). In contrast, previous studies showed that, using a nonrelativistic approximation, i.e., BP(NR)[32] or LDA(NR),[33] one can get a seemingly correct magnetic moment and bond length, but the dissociation energy is still at least 30% too large. Apparently, using a hybrid XC functional or a nonrelativistic approximation improves the DFT results.

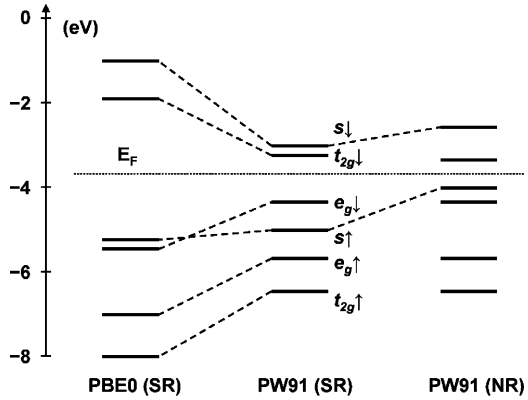

Figure 1. Atomic levels of a single Ru atom calculated in DFT with PBE0(SR), PW91(SR), and PW91(NR).

To reveal the origin of the improvement of the DFT results using a hybrid XC functional and the apparent improvement using a nonrelativistic approximation, we study the atomic levels of a single Ru atom in detail. The resulting ground-state electronic configuration of a free Ru atom is $4d^7 5s^1$, or $^5F_5$, as experimentally determined. Thus, DFT can give the correct ground state for a Ru atom. The fivefold degenerate 4d levels split into threefold degenerate t_{2g} and twofold degenerate e_g levels. In Figure 1, from left to right, three sets of atomic level calculated with PBE0(SR), PW91(SR), and PW91(NR) for a free Ru atom are shown schematically according to the energy scale.

For PW91(SR) (central column of Figure 1), used by Zhang et al.,[2] from low to high energy, the spin-up t_{2g}, e_g, and s levels are fully occupied, while only the spin-down e_g levels are occupied. So, there are four unpaired electrons, and the total magnetic moment is 4 μ_B. The spin-down e_g levels are the highest occupied levels at −4.24 eV, and the spin-down t_{2g} levels are the lowest unoccupied levels at −3.43 eV. The corresponding gap is 0.81 eV. Table 2 lists the relative positions of the atomic levels calculated using PW91 or PBE versions of GGA(SR) for various implementations of DFT, and all results agree with each other, as they should. The spin-up e_g levels are about 0.7 eV above the spin-up t_{2g} levels, the spin-down e_g levels are about 1.3 eV above the spin-up e_g levels, and the spin-up s level is about 0.8 eV above the spin-up e_g levels.

TABLE 2: Relative Positions of Ru Atomic Levels Calculated Using DFT-GGA with Scalar Relativistic Effects

	VASP PW91(SR)	NWC PW91(SR)	FLAIR PW91(SR)	NRL-MOL PBE(SR)
$s^{\uparrow} - e_g^{\uparrow}$	0.83	0.81	0.82	0.73
$e_g^{\downarrow} - e_g^{\uparrow}$	1.39	1.28	1.32	1.33
$e_g^{\uparrow} - t_{2g}^{\uparrow}$	0.66	0.77	0.71	0.72

TABLE 3: Relative Positions of Ru Atomic Levels Calculated Using DFT-PBE0 with Scalar Relativistic Effects and DFT-GGA with Nonrelativistic Approximation

	NWC PBE0(SR)	FLAIR PW91(NR)	NRL-MOL PBE(NR)
$s^{\uparrow} - e_g^{\uparrow}$	1.65	1.52	1.48
$e_g^{\downarrow} - e_g^{\uparrow}$	1.48	1.29	1.30
$e_g^{\uparrow} - t_{2g}^{\uparrow}$	0.65	0.73	0.73

For PBE0 (left column of Figure 1), which incorporates 25% exact exchange, we repeated the calculation for a single Ru atom using NWChem. In comparison with the PW91(SR) results, the occupied and unoccupied levels are shifted toward lower and higher energies, respectively. Among them, the spin-down s level is shifted the smallest and becomes the highest occupied level with the eigenvalue of −5.22 eV. The corresponding gap is now 3.36 eV, much larger than the GGA(SR) result, as expected from the hybrid XC functional. The relative positions of the atomic levels are listed in Table 3. The spin-up e_g levels are 0.65 eV above the spin-up t_{2g} levels, and the spin-down e_g levels are 1.48 eV above the spin-up e_g levels. These relative positions are not much different from those calculated using GGA(SR). However, the spin-up s level is now 1.65 eV above the spin-up e_g levels, which is twice as large as that in GGA-(SR). Thus, the largest change is the relative position of spin-up s level with respect to e_g levels.

By turning off the relativistic effects (which is not possible in all the codes), we did all-electron calculations using FLAIR and NRL-MOL with PW91 and PBE, respectively. The results are shown in the right column of Figure 1 and Table 3. As shown in Figure 1, the absolute positions of t_{2g} and e_g levels change very little. Only the s levels are shifted up toward higher energy, as expected when scalar relativistic (Darwin, and to a less extent, mass−velocity) effects are removed. The spin-up s level is above the spin-down e_g levels and becomes the highest occupied level at −4.08 eV. The corresponding gap is 0.50 eV, which is smaller than the scalar relativistic result. As listed in Table 3, the only significant change is that the spin-up s level is now 1.5 eV above the spin-up e_g levels, which is similar to the PBE0(SR) results, but not for the same physical reasons. To be more specific, throwing away the scalar relativistic effects (predominately, given by Darwin term) affects the absolute value of the s level, as shown in the right column of Figure 1 compared to the central column, whereas correcting the electron self-interaction error changes the absolute values of all the d and s levels, as shown in the left column of Figure 1 for PBE0. Thus, as discussed next, the net result is that both the correct PBE0-(SR) and incorrect GGA(NR) descriptions attain a similar e_g−s hybridization, which is different from GGA(SR).

A Ru dimer has $D_{\infty h}$ symmetry. Hence, among the d orbitals, only the $e_g(d_{z^2})$ orbital is subjected to hybridization with an s orbital. As mentioned above and shown in Figure 1, when PBE0 (or GGA nonrelativistic approximation) is used, the largest change is that the separation between spin-up s level and e_g levels is increased by 0.8 eV, in comparison with GGA(SR) results. So, the overestimation of energy gain from $e_g(d_{z^2})$−s hybridization in GGA(SR) is corrected by removing electron self-interaction via, for example, PBE0, which give results in good agreement with MRSDCI calculations for Ru_2, and fictitiously corrected by ignoring relativistic effects.

TABLE 4: Magnetic Moment (M) and Atomization Energy (E_a) Calculated in DFT using PBE0(SR) and PW91(SR) for Ru Tetramer (Ru_4) in Square and Tetrahedron Structures[a]

	M (μ_B)	E_a (eV)
	NWC PBE0(SR)	
square	4	5.52
tetrahedron	8	6.20
	VASP PW91(SR)	
square	4	12.32
tetrahedron	2 (4)	11.78 (11.41)
	VASP PW91(SR)[2]	
square	4	12.36
tetrahedron	4	11.24

[a] For PW91(SR), we show in parentheses that $M = 4\mu_B$ is metastable for the tetrahedron, in contrast to the results from ref 2. Again, as for dimer (see Table 1), bonding is changed because of the semicore contribution.

As to the ground state of the Ru tetramer (Ru_4), there is neither experimental data nor high-level quantum chemistry calculation. As shown in Table 4, PW91(SR) gives the square structure as the ground state with the magnetic moment of 4 μ_B and the atomization energy of 12.32 eV. The tetrahedron structure is 0.54 eV lower in atomization energy with a magnetic moment of 2 μ_B. The preference of the square structure of PW91(SR) agrees with the calculations by Zhang et al.[2] The relaxed structures are shown in Figure 2 a,b. The Ru−Ru bond lengths in the square structure are almost the same at 2.26 Å. The difference is less than 0.002 Å, which shows that there is a very small Jahn−Teller distortion. The tetrahedron structure is distorted from the perfect T_d symmetry, and the Ru−Ru bond lengths range from 2.26 to 2.72 Å. However, with its greatly reduced unphysical self-interaction of electrons, PBE0(SR) gives the tetrahedron as the ground-state structure with a larger magnetic moment of 8 μ_B and reduced atomization energy of 6.20 eV. The preference of a tetrahedron over a square is 0.68 eV. Figure 2c shows that the structure is distorted with PBE0-(SR) from the D_{4h} symmetry and the bond length ranges from 2.29 to 2.36 Å. The tetrahedron structure is also distorted, and the bond length ranges from 2.32 to 2.73 Å. The trend of higher magnetic moment, longer bond length, and smaller atomization energy for the Ru tetramer with PBE0(SR) than PW91(SR) is consistent with the results for the Ru dimer.

Importantly, the preference of the tetrahedron structure for the Ru tetramer can also be explained by the electronic structure of a single Ru atom. As mentioned above, the largest difference between PBE0(SR) and PW91(SR) results is the much higher position of the spin-up s level with respect to the spin-up e_g levels. As shown in Figure 3, the square (D_{4h} symmetry) and tetrahedron (T_d symmetry) structures are highlighted on an fcc lattice. According to symmetry, only the $e_g(d_{z^2})$ orbital can hybridize with an s orbital in a square configuration, not a tetrahedron. The hybridization between t_{2g} and s orbitals is negligible because of the large separation between them in energy. For PW91(SR), the square has lower energy, because the spin-up $e_g(d_{z^2})$−s hybridization is strong and $e_g(d_{x^2-y^2})$−e_g-$(d_{x^2-y^2})$ interaction favors second nearest-neighbor bonds, as shown in the top of Figure 3. In distinct contrast, for PBE0-(SR), the spin-up s level now lies much higher above the spin-up e_g levels, so the $e_g(d_{z^2})$−s hybridization is much weaker, and thus, the tetrahedron is favored.

Finally, Guo and Balasubramanian[34] recently carried out an MRSDCI calculation for the Ru trimer (Ru_3). They found that

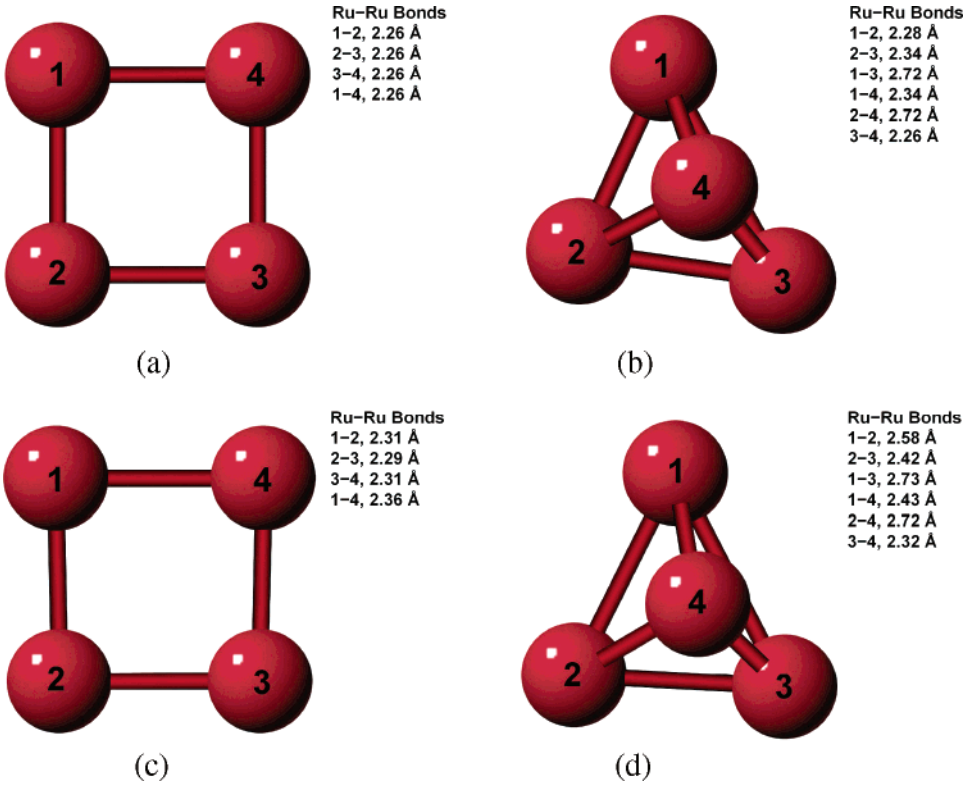

Figure 2. Square and tetrahedron for Ru tetramer calculated with PW91(SR) (a and b) and PBE0(SR) (c and d), which have much larger bond lengths. Numbers label atoms and bonds, with bond lengths listed.

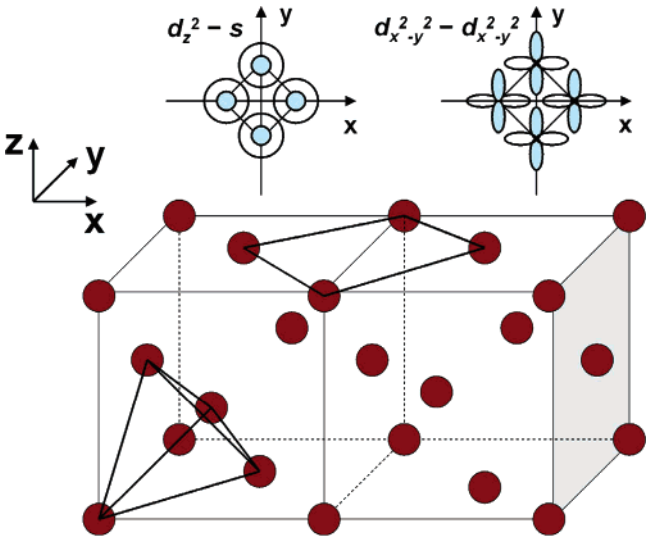

Figure 3. Square (D_{4h}) and tetrahedron (T_d) structures for Ru tetramer (Ru_4) relative to an fcc lattice. The $e_g(d_{z^2})-s$ and $d_{x^2-y^2}-d_{x^2-y^2}$ bonding interactions for the square are shown at the top. The bright (dark) areas mean positive (negative) phases of the orbitals.

the ground state is $^{11}B_1$ with 10 μ_B, in an isosceles triangle structure, and the atomization energy is 6.16 eV. As shown in Table 5, the short bond is 2.67 Å, and the angle between two short bonds is 94.3°. They also did DFT calculations with a hybrid XC functional, B3LYP,[13] which gives the ground state with 8 μ_B in an equilateral triangle structure with bond length of 2.42 Å. In this study, the PBE0(SR) results for Ru_3 are very close to those with B3LYP(SR), as should be expected; however, the calculated atomization energy is 20% smaller than the MRSDCI result. In contrast, as shown in Table 5, we found that PW91(SR) gives an even smaller magnetic moment and

TABLE 5: Magnetic Moment (M), Atomization Energy (E_a), and Structure for Ru Trimer (Ru_3)[a]

	M (μ_B)	E_a (eV)	R (Å)	θ (deg)
MRSDCI[34]	10	6.16	2.67	94.3
B3LYP (SR)[34]	8		2.42	60.0
PBE0 (SR)	8	4.91	2.45	60.4
PW91 (SR)	6	7.82	2.28	65.3
PW91 (SR)[2]	6	7.77	2.20	65.2

[a] The structure is specified by shorter bond (R) and the angle (θ) between the shorter bonds. For differences with the results from ref 2, see captions of Tables 1 and 4.

bond lengths and a much larger atomization energy, which is in the same trend as we found for Ru_2 and Ru_4.

The improvement of magnetic moment, bond length, and atomization energy of PBE0(SR) for Ru_3 with respect to PW91-(SR) are again the result of the larger separation of spin-up s and e_g levels. However, PBE0(SR) overcorrect the atomization energy with respect to the MRSDCI value. This shows that the correct ground-state structure for the Ru trimer depends very sensitively on the position of s with respect to the e_g levels. Although the hybrid XC functional can correct the positions of the s level to some extent, a precise determination requires high-level quantum chemistry methods, which treat strong electron correlation effects more accurately.

Conclusion

In conclusion, ground-state structures of small Ru clusters have been studied carefully. We have shown that the PBE0 hybrid exchange-correlation functional, which includes partially exact exchange, corrects much of the structural and binding errors for the Ru dimer, in agreement with experimental and MRSDCI results. Importantly, the ground-state structure of the Ru tetramer is a tetrahedron, not a square. We have shown that the DFT-GGA preference of square and cubic ground-state

structures for small Ru clusters previously reported by Zhang et al.[2] was a consequence of unphysical electron self-interaction. The change of Ru_4 structural preference to the tetrahedron can be explained by the electronic structure of a single Ru atom and is due to the relative position of the spin-up s level with respect to the e_g levels. We also showed how the standard DFT-GGA without including the relativistic effects gives similar results as the hybrid exchange-correlation functionals—akin to "the right results for the wrong reasons". Our results again highlight the need to validate DFT methods for their application in nanoscience.

Acknowledgment. We thank Mark Pederson for use of NRMOL. This work was supported by the Department of Energy under Catalysis DE-FG02-03ER15476 and The Frederick Seitz Materials Research Laboratory at the University of Illinois under DEFG02-91ER45439. We also acknowledge computational support provided by the Materials Computation Center through NSF/ITR grant DMR-0325939.

References and Notes

(1) Landgrebe, A. R., Sen, R. K., Wheeler, D. J., Eds.; *Proceedings of the Workshop on Direct Methanol-Air Fuel Cells*; Electrochemical Society: Washington, DC, 1992; Vol. 92−14.

(2) Zhang, W. Q.; Zhao, H. T.; Wang, L. C. *J. Phys. Chem. B* **2004**, *108*, 2140−2147.

(3) Perdew, J. P.; Emzerhof, M.; Burke, K. *J. Chem. Phys.* **1996**, *105*, 9982−9985.

(4) Adamo, C.; Barone, V. *J. Chem. Phys.* **1999**, *110*, 6158−6170.

(5) Svane, A.; Gunnarsson, O. *Phys. Rev. Lett.* **1990**, *65*, 1148−1151.

(6) Perdew, J. P.; Zunger, A. *Phys. Rev. B* **1981**, *23*, 5048−5079.

(7) Pederson, M. R.; Heaton, R. A.; Lin, C. C. *J. Chem. Phys.* **1985**, *82*, 2688−2699.

(8) Sharp, R. T.; Horton, G. K. *Phys. Rev.* **1953**, *90*, 317.

(9) Grabo, T.; Kreibich, T.; Kurth, S.; Gross, E. K. U. In *Strong Coulomb Correlations in Electronic Structure: Beyond the Local Density Approximation*; Anisimov, V. I., Ed.; Gordon & Breach: Tokyo, 1998.

(10) Talman, J. D.; Shadwick, W. F. *Phys. Rev. A* **1976**, *14*, 36.

(11) Casida, M. E. In *Recent Developments and Applications of Density Functional Theory*; Seminario, J. M., Ed.; Elsevier: Amsterdam, 1996; p 391.

(12) Becke, A. D. *J. Chem. Phys.* **1993**, *98*, 1372−1377.

(13) Becke, A. D. *J. Chem. Phys.* **1993**, *98*, 5648−5652.

(14) Becke, A. D. *J. Chem. Phys.* **1996**, *104*, 1040−1046.

(15) Adamo, C.; Scuseria, G. E.; Barone, V. *J. Chem. Phys.* **1999**, *111*, 2889−2899.

(16) Adamo, C.; Barone, V. *Theor. Chem. Acc.* **2000**, *105*, 169−172.

(17) Vetere, V.; Adamo, C.; Maldivi, P. *Chem. Phys. Lett.* **2000**, *325*, 99−105.

(18) Guillemoles, J. F.; Barone, V.; Joubert, L.; Adamo, C. *J. Phys. Chem. A* **2002**, *106*, 11354−11360.

(19) Ciofini, I.; Laine, P. P.; Bedioui, F.; Adamo, C. *J. Am. Chem. Soc.* **2004**, *126*, 10763−10777.

(20) Franchini, C.; Bayer, V.; Podloucky, R.; Paier, J.; Kresse, G. *Phys. Rev. B* **2005**, *72*, 045132.

(21) Kresse, G.; Furthmüller, J. *Comput. Mater. Sci.* **1996**, *6*, 15−50.

(22) Kresse, G.; Furthmüller, J. *Phys. Rev. B: Condens. Matter* **1996**, *54*, 11169−11186.

(23) Weinert, M.; Wimmer, E.; Freeman, A. J. *Phys. Rev. B* **1982**, *26*, 4571−4578.

(24) Wimmer, E.; Krakauer, H.; Weinert, M.; Freeman, A. J. *Phys. Rev. B* **1981**, *24*, 864−875.

(25) Kendall, R. A.; Apra, E.; Bernholdt, D. E.; Bylaska, E. J.; Dupuis, M.; Fann, G. I.; Harrison, R. J.; Ju, J. L.; Nichols, J. A.; Nieplocha, J.; Straatsma, T. P.; Windus, T. L.; Wong, A. T. *Comput. Phys. Commun.* **2000**, *128*, 260−283.

(26) Pacific Northwest National Laboratory, Richland, WA 99352-0999; 2005.

(27) Pederson, M. R.; Jackson, K. A. *Phys. Rev. B* **1990**, *41*, 7453−7461.

(28) Jackson, K.; Pederson, M. R. *Phys. Rev. B* **1990**, *42*, 3276−3281.

(29) Das, K. K.; Balasubramanian, K. *J. Chem. Phys.* **1991**, *95*, 2568−2571.

(30) Wang, H. M.; Liu, Y. F.; Haouari, H.; Craig, R.; Lombardi, J. R.; Lindsay, D. M. *J. Chem. Phys.* **1997**, *106*, 6534−6537.

(31) We note that ref 2 incorrectly cites D_e as eV/atom, whereas it is really the total dissociation energy in ref 29.

(32) Harada, M.; Dexpert, H. *J. Phys. Chem.* **1996**, *100*, 565−572.

(33) Andzelm, J.; Radzio, E.; Salahub, D. R. *J. Chem. Phys.* **1985**, *83*, 4573−4580.

(34) Guo, R.; Balasubramanian, K. *J. Chem. Phys.* **2003**, *118*, 142−148.